Distillation of The Two-Mode Squeezed State

Yury Kurochkin
Russian Quantum Centre, 100 Novaya Street, Skolkovo, Moscow 143025, Russia

Adarsh S. Prasad
Institute for Quantum Science and Technology, University of Calgary, Alberta T2N1N4, Canada

A. I. Lvovsky
Russian Quantum Centre, 100 Novaya Street, Skolkovo, Moscow 143025, Russia
and Institute for Quantum Science and Technology, University of Calgary, Alberta T2N1N4, Canada
(Received 29 July 2013; published 20 February 2014)

We experimentally demonstrate entanglement distillation of the two-mode squeezed state obtained by parametric down-conversion. Applying the photon annihilation operator to both modes, we raise the fraction of the photon-pair component in the state, resulting in the increase of both squeezing and entanglement by about 50%. Because of the low amount of initial squeezing, the distilled state does not experience significant loss of Gaussian character.

DOI: 10.1103/PhysRevLett.112.070402 PACS numbers: 03.65.Wj, 03.65.Ta, 42.50.Xa

Entanglement is paramount in quantum technology. However, entangled states are difficult to prepare and vulnerable to decoherence and losses. This issue is particularly significant in quantum optical communications where entanglement needs to be distributed over long distances.

It can be addressed using entanglement distillation (ED) [1], a procedure in which the parties use classical communications and local operations to obtain, from a set of entangled states, a smaller set of states with a higher level of entanglement. ED has been successfully demonstrated in the discrete-variable domain [2,3]. But for continuous-variable (CV) quantum-information processing, ED is complicated because of a no-go theorem [4–6] that prohibits distillation of a Gaussian entangled state by any Gaussian operations. Gaussian operations include phase-space displacement, squeezing, application of beam splitters, homodyne detection—i.e., such operations that preserve the Gaussian character of a state's Wigner function and are typical for CV processing. The primary continuous-variable entangled resource, the two-mode squeezed vacuum (TMSV), is Gaussian [7], so one must leave the boundaries of the the CV domain in order to distill it. This is the purpose of the present work.

TMSV is of special value for quantum science and technology [7]. Thanks to nonclassical correlation of quadrature observables of the two modes, this state constitutes a physically plausible approximation of the original Einstein-Podolsky-Rosen state [8] that triggered the quantum nonlocality debate. In addition to fundamental interest, TMSV is the basis of complete quantum teleportation [9] and CV quantum repeaters [10], as well as certain quantum metrology [11] and quantum key distribution [12,13] applications. Hence, it is important to develop and test a reliable procedure for the distillation of that state.

A non-Gaussian operation that has been extensively discussed in the context of CV ED is the photon annihilation operator $\hat{a}$. It is realized by reflecting the target optical mode from a low transmissivity beam splitter with the single-photon detector placed in its transmitted channel. Registration of a photon heralds photon annihilation in the reflected channel. This operation was first implemented by Wenger *et al.* [14] and has since been used in a number of CV quantum engineering experiments [15,16].

Entanglement distillation of the TMSV with photon annihilation was first proposed by Opartný *et al.* [17] and further theoretically investigated for photon-number resolving [18] and threshold detectors [19]. A comprehensive theoretical analysis in Ref. [20] considered different types of detectors and realistic noisy measurements.

CV entanglement increase by photon annihilation has been demonstrated experimentally, but in none of the existing experiments did the resulting state retain the two-mode squeezing property, i.e., simultaneous correlation of positions and anticorrelation of momenta beyond the vacuum level. Ourjoumtsev *et al.* applied nonlocal photon subtraction to TMSV, resulting in a state that approximates the delocalized single photon [21,22]. CV ED employing two-mode photon annihilation was demonstrated for Gaussian input states created by equal splitting of a single-mode squeezed state in Ref. [23]. In that work, entanglement increase has been observed along with enhanced nonclassical quadrature correlations for specific values of the phase difference between the two modes. In another set of experiments, artificial non-Gaussian disturbance has been applied to a TMSV, resulting in a loss of its Gaussian character. Subsequently, the

entanglement was distilled by means of a Gaussian process [24,25], but not beyond the entanglement level of the original TMSV.

We now proceed to explaining the idea of our work in an idealized, loss-free setting. TMSV is obtained by applying the two-mode squeezing operator $S(\zeta) = e^{\zeta(\hat{a}_1\hat{a}_2 - \hat{a}_1^\dagger\hat{a}_2^\dagger)}$ (where ζ is the real squeezing parameter) to modes 1 and 2 initially in the vacuum state [26]. It has the following representation in the photon number basis:

$$|\Psi\rangle = S(\zeta)|0,0\rangle = \sqrt{1-\lambda^2}\sum_{n=0}^{\infty}\lambda^n|n,n\rangle, \tag{1}$$

for $\lambda = \tanh\zeta$. If we apply annihilation operators to both modes of $|\Psi\rangle$, we find

$$\hat{a}_1\hat{a}_2|\Psi\rangle = \sqrt{1-\lambda^2}\sum_{n=1}^{\infty} n\lambda^n|n-1,n-1\rangle. \tag{2}$$

In the limit of small squeezing, both states (1) and (2) can be approximated to its first order. After renormalization, we find

$$|\Psi\rangle \approx |0,0\rangle + \lambda|1,1\rangle, \tag{3}$$

$$\hat{a}_1\hat{a}_2|\Psi\rangle \approx |0,0\rangle + 2\lambda|1,1\rangle. \tag{4}$$

A higher contribution of the photon-pair term causes the enhancement of both entanglement and two-mode squeezing [20].

The price to pay for this enhancement is the loss of the state's Gaussian character. This is because the higher-number terms in Eq. (2) do not follow the pattern (1) of the TMSV. However, the emerging non-Gaussianity does not preclude improved capacity of that state as a resource for quantum teleportation [17–19], quantum dense coding [27], quantum key distribution [28], and quantum metrology [29]. In fact, it opens up new applications: for example, the distilled (non-Gaussian) state can be used to demonstrate quantum nonlocality by means of homodyne detection [30–32]. In our experiment, however, the loss of Gaussian character is negligible because the down-conversion amplitude λ is relatively low, so the higher-number terms do not play a significant role.

In the ideal case, entanglement distillation is also expected if photon annihilation is applied to only one of the modes of the initial TMSV:

$$\hat{a}_1|\Psi\rangle \approx |0,1\rangle + \sqrt{2}\lambda|1,2\rangle. \tag{5}$$

However, this state no longer has the form of TMSV and is not expected to feature nonclassical quadrature correlation. Furthermore, as we see below, in our experiment, state $\hat{a}_1|\Psi\rangle$ does not exhibit increased entanglement because of the losses.

A signature feature of two-mode squeezing is the correlation of quadrature measurement statistics. In the two modes, the position and momentum observables are, respectively, correlated and anticorrelated beyond the level allowed by the uncertainty principle for separable states:

$$\langle (X_1 \mp X_2)^2\rangle = e^{\mp 2\zeta},$$
$$\langle (P_1 \mp P_2)^2\rangle = e^{\pm 2\zeta}.$$

For quadrature observables $X(\theta) = X\cos\theta + P\sin\theta$ associated with arbitrary phases in the two modes, the correlated variance takes the form

$$\langle [X_1(\theta_1) \pm X_2(\theta_2)]^2\rangle = \{(1-\eta) + \eta[\cosh(2\zeta) \pm \cos(\theta_1+\theta_2)\sinh(2\zeta)]\}, \tag{6}$$

where we have taken into account the optical loss $1-\eta$ in both modes. Remarkably, the correlation depends only on the sum but not the difference of the phases in the two modes. This feature can be understood by reviewing the photon number decomposition (1) of TMSV. A phase shift by angle θ in a single mode corresponds to operator $e^{i\theta\hat{n}}$, where $\hat{n}$ is the photon number operator. Because all terms of Eq. (1) contain equal photon numbers in both modes, a change in $\theta_1 - \theta_2$ for constant $\theta_1 + \theta_2$ implies an equal and opposite quantum phase shift of the two modes, and will leave the state unchanged. This characteristic feature of TMSV is preserved in our ED protocol, in contrast to previous photon subtraction CV ED experiments [21–23].

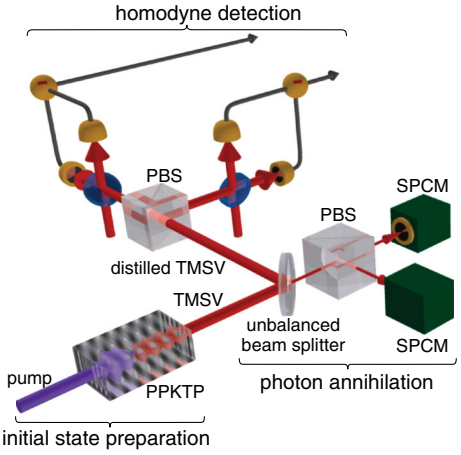

FIG. 1 (color online). Experimental setup. Type II parametric down-conversion in a PPKTP crystal generates the two-mode squeezed vacuum state in two polarization modes. Each mode is subjected to the annihilation operator realized by an unbalanced beam splitter and a single photon detector. The prepared distilled two-mode squeezed state has higher squeezing and entanglement, as verified by homodyne detection. SPCM, single-photon counting module; PBS: polarizing beam splitter.

In our experiment (Fig. 1), we generate a TMSV using nondegenerate parametric down-conversion and perform multiple quadrature measurements in both modes of the original and distilled states. The acquired data allow us to verify entanglement distillation in two ways. First, we evaluate the phase-dependent variance of the sum and difference of the quadratures acquired in the two modes and verify that the minimal value of that variance decreases after distillation, corresponding to a higher squeezing. Second, we use the complete set of quadrature data for full characterization of the original and distilled states by means of homodyne tomography [15]. We then verify the entanglement increase by evaluating, for both states, the log-negativity value $E_N = \log_2(1 + 2N)$, where negativity N is the entanglement monotone [33] equal to the sum of absolute values of negative eigenvalues of the state's partially transposed density matrix. For Gaussian states, the log negativity is a proper measure of entanglement [34].

The experimental setup is presented in Fig. 1. The two-mode squeezed state is prepared by a type II spontaneous parametric down-conversion in a periodically-poled potassium-titanyl phosphate (PPKTP) crystal in a spatially and spectrally degenerate but polarization-nondegenerate configuration. The PPKTP crystal is pumped by 395-nm wavelength pulses generated by doubling 790-nm pulses from a master Ti:sapphire mode-locked laser, with a repetition rate of 76 MHz and pulse width 1.6 ps. The down-conversion is followed by a polarization-independent beam splitter with 11% transmissivity. The transmitted signal is subjected to narrow-band spectral filtering, after which it is separated according to polarization and each mode is subjected to single photon detection. PerkinElmer SPCM-AQR-14-FC detectors, coupled through single-mode fibers, are used [35]. In spite of non-negligible two-mode squeezing and an over 50% efficiency of the detectors, the coincidence photon count rate is only ~100 Hz because of the losses associated with the spatial and spectral filtering [36]. The light reflected from the beam splitter is separated into the two TMSV modes by a polarizing beam splitter and each mode is subjected to homodyne measurements [37]. The local oscillators for the balanced homodyne detectors are derived from the master laser.

Photon annihilation events correspond to "clicks" of photon detectors in the relevant mode. Events without detector clicks correspond to the initial TMSV $|\Psi\rangle$ and are used to measure the local oscillator phases as well as quantify initial squeezing and entanglement. Simultaneous clicks in both detectors herald the distilled TMSV state, for which we observe the squeezing and entanglement increase.

A detector click in only one of the modes (e.g., mode 1) leads to the one-photon subtraction state (5) which approximates, in the limit of low squeezing, a tensor product of the vacuum and single-photon states. In the presence of losses, the state of mode 2 becomes a mixture of the single-photon and vacuum states. Reconstructing the state of that mode permits precise evaluation of the loss present in the experiment as $1 - \eta = 0.58 \pm 0.01$ [38]. This figure includes the 11% loss from the beam splitter used for photon subtraction.

We allow the local oscillator phase in one of the homodyne detectors to fluctuate freely with air movements while that in the other channel is varied with a period of about 1 s by means of a piezoelectric transducer. With each heralding event, we acquire a single pair of quadratures associated with that event plus a series of 9500 quadrature pairs associated with subsequent (not heralded) laser pulses. We can safely assume the local oscillator phases to be constant during that acquisition. Because the output of the

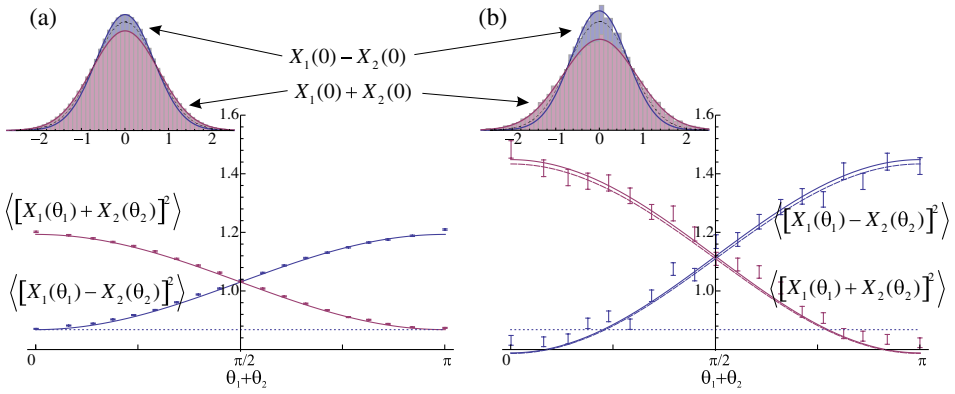

FIG. 2 (color online). Variances of the sum and difference of the quadratures measured in the two modes: (a) unconditionally, (b) conditioned on photon annihilation events in both channels. The noise level corresponding to the double vacuum state is 1. The solid line in (a) is the fit based on a lossy TMSV model with the squeezing parameter of $\zeta = 0.19$; the solid line in (b) is a theoretical prediction based on the fit in (a) and photon annihilation applied in both modes. The dashed line in (b) corresponds to a TMSV model with increased squeezing parameter $\zeta = 0.358$ that has experienced the same loss as the state in (a). The dotted line in both panels corresponds to the highest level of squeezing in the unconditionally measured state, according to the fit. The insets show histograms of the sum and difference of the position quadratures corresponding to each case. The dashed line shows the standard quantum limit. Enhancement of squeezing is present in (b) while the loss of Gaussian character is insignificant.

parametric down-conversion is a two-mode squeezed state, the correlated quadrature variance $\langle[X_1(\theta_1)\mp X_2(\theta_2)]^2\rangle$ in each series provides us with the information on the sum of the local oscillator phases $(\theta_1+\theta_2)$ in accordance with Eq. (6).

A plot of the measured variance of $\langle[X_1(\theta_1)\mp X_2(\theta_2)]^2\rangle$ versus phase $\theta_1+\theta_2$ is presented in Fig. 2 for both nonheralded [2(a)] and heralded [2(b)] measurements. They correspond to states $|\Psi\rangle$ and $\hat{a}_1\hat{a}_2|\Psi\rangle$, respectively. Minimum variances $\langle[X_1(\theta_1)-X_2(\theta_2)]^2\rangle$ and $\langle[X_1(\theta_1)+X_2(\theta_2)]^2\rangle$ at local oscillator phases $\theta_1+\theta_2$ being 0 and π, respectively, fall below the standard quantum limit, which indicates squeezing. We observe an increase of squeezing from 0.560 ± 0.005 dB for the undistilled state to 0.83 ± 0.05 dB for the distilled state.

As expected for a TMSV with a small initial amount of squeezing, the distilled state does not exhibit strong deviation from the Gaussian shape [Fig. 2(b), inset]. This can be quantified by evaluating the fourth moment of the quadrature probability distributions. For example, for $\theta_1+\theta_2=0$, the fourth moments of $X_1(\theta_1)-X_2(\theta_2)$ and $X_1(\theta_1)+X_2(\theta_2)$ are 0.522 ± 0.010 and 1.532 ± 0.028, whereas the fourth moments expected from Gaussian distributions with the same variances are 0.516 and 1.532, respectively.

For higher precision analysis, we fit the data in Fig. 2(a) by the model of quadrature variance dependence (6) for a TMSV with the value of η found previously. From that fit, we evaluate the initial TMSV squeezing parameter, prior to losses, as $\zeta=0.190$. If we subject this TMSV to two-mode photon annihilation operation, we obtain theoretical curves shown by solid lines in Fig. 2(b), which turn out to well match the experimental data.

Taking advantage of the almost Gaussian nature of the distilled state, we fit its measured variances [Fig. 2(b)] by a TMSV with an increased squeezing parameter $\zeta=0.358$ that has undergone the same losses as the initial state [dashed lines in Fig. 2(b)]. Good agreement is obtained, indicating that the state has retained its two-mode squeezed character after distillation.

From the quadrature measurements we reconstruct density matrices of both the initial and final states in the Fock basis up to three photons by means of the maximum-likelihood method [39,40]. Absolute values of the lowest density matrix elements are presented in Figs. 3(a) and 3(b). The off-diagonal components $|0,0\rangle\langle1,1|$ and $|1,1\rangle\langle0,0|$ in the final state are significantly greater than those in the initial state, serving as evidence of higher entanglement. For a more rigorous estimation of the entanglement increase, we evaluate the log-negativity parameter E_N from the reconstructed density matrices and list it in Table I. An increase by a factor of about 50% is present.

In an ideal setting, as seen from Eq. (5), we would also expect entanglement increase in the case of single-mode photon annihilation. However, in the presence of losses, the one-photon subtracted state demonstrates lower entanglement compared to initial TMSV (Table I). This is because the

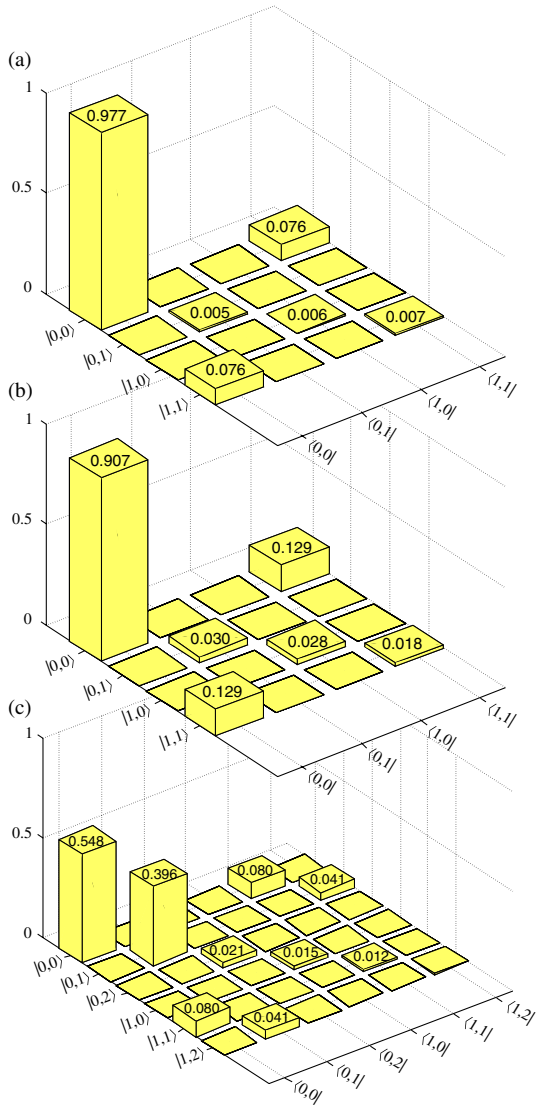

FIG. 3 (color online). Low photon number components of the density matrices (absolute values) reconstructed from the quadrature data sets measured: (a) unconditionally, (b) conditioned on photon annihilation events in both channels, (c) conditioned on photon annihilation event in channel 1. Increase in the off-diagonal elements associated with terms $|0,0\rangle\langle1,1|$ and $|1,1\rangle\langle0,0|$ in (b) compared to (a) is evidence of entanglement distillation. All matrix elements above 0.005 are marked. No compensation for the loss is implemented.

entanglement of that state (5) occurs due to the $|1,2\rangle$ component [Fig. 3(c)], and the two-photon Fock state is highly sensitive to losses, more so than the single-photon state.

For fair evaluation of the distillation procedure, we should correct the parameters obtained for the unheralded state for the loss occurring in the asymmetric beam splitter. The corrected values for the squeezing and entanglement are still significantly below those for the distilled state (Table I).

The entanglement increase factor in the procedure described in this experiment is theoretically limited by 2. More entanglement can be obtained by higher-order photon

TABLE I. Parameters of the states before and after distillation.

State	Squeezing parameter ζ from fit	Maximum squeezing (dB)	Log negativity
Initial TMSV	0.1900 ± 0.0007	0.560 ± 0.005	0.209 ± 0.002
Initial TMSV compensated for beam splitter	0.1900 ± 0.0007	0.63 ± 0.005	0.239 ± 0.002
Two-mode photon subtraction	0.358 ± 0.006	0.83 ± 0.05	0.30 ± 0.01
One-mode photon subtraction	not applicable	not applicable	0.12 ± 0.01

annihilation, but at a cost of dramatic productivity loss. More promising techniques of CV entanglement distillation would involve nonclassical light sources or nonlinear optical interactions in both modes of TMSV. For example, a procedure involving noiseless amplification [41] in both modes has no fundamental limitation on the achievable entanglement increase factor.

The experiment has been supported by NSERC and CIFAR. We thank Marco Barbieri, Alexey Fedorov, Joshua Nunn, Evgeniy Safonov, and Ian Walmsley for helpful discussions.

[1] C. H. Bennett, G. Brassard, S. Popescu, B. Schumacher, J. A. Smolin, and W. K. Wootters, Phys. Rev. Lett. **76**, 722 (1996).
[2] P. G. Kwiat, S. Barraza-Lopez, A. Stefanov, and N. Gisin, Nature (London) **409**, 1014 (2001).
[3] J.-W. Pan, S. Gasparoni, R. Ursin, G. Weihs, and A. Zeilinger, Nature (London) **423**, 417 (2003).
[4] J. Fiurášek, Phys. Rev. Lett. **89**, 137904 (2002).
[5] J. Eisert, S. Scheel, and M. B. Plenio, Phys. Rev. Lett. **89**, 137903 (2002).
[6] G. Giedke and J. I. Cirac, Phys. Rev. A **66**, 032316 (2002).
[7] S. L. Braunstein and P. van Loock, Rev. Mod. Phys. **77**, 513 (2005).
[8] A. Einstein, B. Podolsky, and N. Rosen, Phys. Rev. **47**, 777 (1935).
[9] A. Furusawa, J. L. Sörensen, S. L. Braunstein, C. A. Fuchs, H. J. Kimble, and E. S. Polzik, Science **282**, 706 (1998).
[10] E. T. Campbell, M. G. Genoni, and J. Eisert, Phys. Rev. A **87**, 042330 (2013).
[11] P. M. Anisimov, G. M. Raterman, A. Chiruvelli, W. N. Plick, S. D. Huver, H. Lee, and J. P. Dowling, Phys. Rev. Lett. **104**, 103602 (2010).
[12] L. Madsen, V. Usenko, M. Lassen, R. Filip, and U. Andersen, Nat. Commun. **3**, 1083 (2012).
[13] F. Grosshans and P. Grangier, arXiv:quant-ph/0204127.
[14] J. Wenger, R. Tualle-Brouri, and P. Grangier, Phys. Rev. Lett. **92**, 153601 (2004).
[15] A. I. Lvovsky and M. G. Raymer, Rev. Mod. Phys. **81**, 299 (2009).
[16] R. Kumar, E. Barrios, C. Kupchak, and A. I. Lvovsky, Phys. Rev. Lett. **110**, 130403 (2013).
[17] T. Opatrný, G. Kurizki, and D.-G. Welsch, Phys. Rev. A **61**, 032302 (2000).
[18] P. T. Cochrane, T. C. Ralph, and G. J. Milburn, Phys. Rev. A **65**, 062306 (2002).
[19] S. Olivares, M. G. A. Paris, and R. Bonifacio, Phys. Rev. A **67**, 032314 (2003).
[20] T. J. Bartley, P. J. D. Crowley, A. Datta, J. Nunn, L. Zhang, and I. Walmsley, Phys. Rev. A **87**, 022313 (2013).
[21] A. Ourjoumtsev, A. Dantan, R. Tualle-Brouri, and P. Grangier, Phys. Rev. Lett. **98**, 030502 (2007).
[22] A. Ourjoumtsev, F. Ferreyrol, R. Tualle-Brouri, and P. Grangier, Nat. Phys. **5**, 189 (2009).
[23] H. Takahashi, J. S. Neergaard-Nielsen, M. Takeuchi, M. Takeoka, K. Hayasaka, A. Furusawa, and M. Sasaki, Nat. Photonics **4**, 178 (2010).
[24] B. Hage, A. Samblowski, J. Diguglielmo, A. Franzen, J. Fiurasek, and R. Schnabel, Nat. Phys. **4**, 915 (2008).
[25] R. Dong, M. Lassen, J. Heersink, C. Marquardt, R. Filip, G. Leuchs, and U. L. Andersen, Nat. Phys. **4**, 919 (2008).
[26] A. I. Lvovsky, arXiv:1401.4118.
[27] A. Kitagawa, M. Takeoka, K. Wakui, and M. Sasaki, Phys. Rev. A **72**, 022334 (2005).
[28] P. Huang, G. He, J. Fang, and G. Zeng, Phys. Rev. A **87**, 012317 (2013).
[29] R. Carranza and C. C. Gerry, J. Opt. Soc. Am. B **29**, 2581 (2012).
[30] H. Nha and H. J. Carmichael, Phys. Rev. Lett. **93**, 020401 (2004).
[31] R. García-Patrón, J. Fiurášek, N. J. Cerf, J. Wenger, R. Tualle-Brouri, and P. Grangier, Phys. Rev. Lett. **93**, 130409 (2004).
[32] R. García-Patrón, J. Fiurášek, and N. J. Cerf, Phys. Rev. A **71**, 022105 (2005).
[33] M. B. Plenio, Phys. Rev. Lett. **95**, 090503 (2005).
[34] K. Audenaert, M. B. Plenio, and J. Eisert, Phys. Rev. Lett. **90**, 027901 (2003).
[35] S. R. Huisman, N. Jain, S. A. Babichev, F. Vewinger, A. N. Zhang, S. H. Youn, and A. I. Lvovsky, Opt. Lett. **34**, 2739 (2009).
[36] $\gamma^2 \approx 0.04$ photon pairs per pulse are produced at a 76 MHz pulse repetition rate. Each photon passes the photon subtraction beam splitter with 11% probability. The spatial and spectral filters account for additional ~90% losses for each photon, and the single-photon detector efficiency equals 60%. This results in coincidence clicks on a scale of 100 Hz.
[37] R. Kumar, E. Barrios, A. MacRae, E. Cairns, E. Huntington, and A. Lvovsky, Opt. Commun. **285**, 5259 (2012).
[38] A. I. Lvovsky, H. Hansen, T. Aichele, O. Benson, J. Mlynek, and S. Schiller, Phys. Rev. Lett. **87**, 050402 (2001).
[39] A. I. Lvovsky, J. Opt. B **6**, S556 (2004).
[40] J. Řeháček, Z. Hradil, E. Knill, and A. I. Lvovsky, Phys. Rev. A **75**, 042108 (2007).
[41] G. Y. Xiang, T. C. Ralph, A. P. Lund, N. Walk, and G. J. Pryde, Nat. Photonics **4**, 316 (2010).